Journal of Solid State Chemistry **151,** 286–293 (2000)
doi:10.1006/jssc.2000.8655, available online at http://www.idealibrary.com on IDEAL®

Three Novel Structure Types of Polythiometalates: Syntheses, Structures, and Electrical Properties of $\{[W_4Ag_6S_{16}]\cdot[Ca(DEAC)_6]\}_n$, $\{[W_2Ag_2S_8]\cdot[Zn(4,4'\text{-bipy})_2(DMF)_2(DMSO)_2]\}_n$, and $\{[W_2Ag_2S_8]\cdot[Zn(4,4'\text{-bipy})_2(DMSO)_4]\cdot(DMSO)\}_n$

Chen Ling, Yu Heng, Wu Liming, Du Wenxin, Gao Xiancheng, Lin Ping, Zhang Wenjian, Cui Chuanpeng, and Wu Xintao[1]

State Key Laboratory of Structural Chemistry, Fujian Institute of Research on the Structure of Matter, The Chinese Academy of Sciences, Fuzhou, Fujian 350002, People's Republic of China

Received November 12, 1999; in revised form February 8, 2000; accepted February 18, 2000

Three novel 1-D coordination polythiometalates have been synthesized and characterized by single-crystal X-ray crystallography, and their electrical properties have been studied. Compound $\{[W_4Ag_6S_{16}]\cdot[Ca(DEAC)_6]\}_n$ 1 crystallizes in the monoclinic space group $P2_1/n$ with $a = 13.769(3)$, $b = 11.613(2)$, $c = 24.153(5)$ Å, $\beta = 96.31(3)°$, $V = 3838.7(13)$ Å, and $Z = 2$ with $R(wR2) = 0.0607(0.1338)$, the polymeric anions in 1 feature a novel hanging ladder-like polymeric chain which can also be described as double helical chains bridged by silver atoms. Both compounds $\{[W_2Ag_2S_8]\cdot[Zn(4,4'\text{-bipy})_2(DMF)_2(DMSO)_2]\}_n$ 2 and $\{[W_2Ag_2S_8]\cdot[Zn(4,4'\text{-bipy})_2(DMSO)_4]\cdot(DMSO)\}_n$ 3 are composite polymers which consist of polymeric cations as well as polymeric anions. In 2, two polymeric chains simultaneously exist in the cell unit, one is the zigzag anionic chain, the other is the linear cationic chain. 2 crystallizes in the monoclinic space group $C2/c$ with $a = 8.996(2)$ Å, $b = 21.728(4)$ Å, $c = 21.560(4)$ Å, $\beta = 94.00(3)°$, $V = 4204(2)$ Å^3, and $Z = 8$ with $R(wR2) = 0.0546(0.1556)$. The difference between 2 and 3 is that the latter has a linear anionic chain and a zigzag cationic chain. X-ray crystallography established the monoclinic space group $C2/c$ with $a = 28.8896(2)$, $b = 11.9395(1)$, $c = 16.2341(2)$ Å, $\beta = 122.932(1)°$, $V = 4699.82(8)$ Å^3, and $Z = 8$ with $R(wR2) = 0.0438(0.1166)\cdot 4.50\times10^{-6}$ S cm^{-1}, respectively. Room temperature conductivities of 1, 2 are 2.92×10^{-5}. Thus, compounds 1 and 2 have semiconductor electrical properties. © 2000 Academic Press

Key Words: **semiconductor; heterometalate; polythiometalate; self-assembly.**

INTRODUCTION

Coordination polymers extended in 1, 2, and 3 dimensions have received much attention in the past few years due to their fascinating and potentially useful properties such as catalysis (1) and conductivity (including superconductivity) (2). Compared with the polyoxometalate (3–5), polythiometalate chemistry is still very young (6). W/Ag/S polymeric cluster complexes are still scarce, there are only seven structure types of this kind of compounds: linear chain, such as $[AgWS_4\cdot\gamma\text{-}MePyH]_n$ and $[AgWS_4\cdot NH_3C(CH_2OH)_3\cdot 2DMF]_n$ (7, 8); double chain, $[AgWS_4\cdot NH_3C(CH_2OH)_3\cdot H_2O]_n$ (9); zigzag chain with unequal steps, $[W_4Ag_4S_{16}\cdot 2Ca(DMSO)_6]_n$ (10); loose helical chain, $[W_3Ag_3S_{12}\cdot Nd(DMSO)_8]_n$ (11); single-stranded helical chain: $[W_3Ag_3S_{12}\cdot La(DMAc)_5(H_2O)_3\cdot(DMAc)_4]_n$ (12); one-dimensional chain, $[W_4Ag_5S_{16}\cdot M(DMSO)_8]_n$ (M = La, Nd) (13, 14); and double square unit zigzag chain with an equal step, $\{W_8Ag_{10}S_{32}\cdot[M(DMSO)_8]_2\}_n$ (M = La, Nd) (12). In research on conducting and semiconducting solid in chemistry and physics (15), the unconventional semiconductors have become a fascinating area since these materials exhibit properties similar to artificial systems of conventional semiconductors. The old polymeric MoS_4CuNH_4 is well known to be a good semiconductor since the 1970s (16). A considerable number of investigations on ternary molybdenum chalcogenides of the formula $M_xMo_yX_z$ has been published (M = Pb, Sn, Cu, Ag, etc., X = S, Se, etc.) (17), but there are still few reports about the semiconducting properties of the Mo(W)/Cu(Ag)/S polymer system. Herein we report three new structure types of W/Ag/S polythiometalates: $\{[W_4Ag_6S_{16}]\cdot[Ca(DEAC)_6]\}_n$ (DEAC = N,N'-diethylacetamide) **1**, a novel hanging ladder-like polymeric chain; compounds **2** and **3** are composite polymers $\{[W_2Ag_2S_8]\cdot[Zn(4,4'\text{-bipy})_2(DMF)_2(DMSO)_2]\}_n$ **2** has a zigzag anionic chain and a linear cationic chain, while $\{[W_2Ag_2S_8]\cdot[Zn(4,4'\text{-bipy})_2(DMSO)_4]\cdot(DMSO)\}_n$ **3** has a linear anionic chain and a zigzag cationic chain. The experimental measure shows **1** and **2** have semiconductor behavior.

[1]To whom correspondence should be addressed. E-mail: wxt@ms.fjirsm.ac.cn.

0022-4596/00 $35.00

EXPERIMENTAL

$(NH_4)_2WS_4$ (18) was achieved by published procedure. Other chemicals were used as purchased with A.R. grade. Elemental analyses were performed by the Elemental Analysis Laboratory in our Institute. Infrared spectra (KBr pellets) were recorded on a Nicolet Magna 750 FT–IR spectrometer, and Raman spectra were collected on a Nicolet 910 FT–Raman Laser spectrometer. Electrical conductivities were measured with pressed pellets (two probe) on ZL5-LCR conductometer.

Syntheses

$\{[W_4Ag_6S_{16}]\cdot[Ca(DEAC)_6]\}_n$ **1**. A CH_3CN solution (6 ml) of $AgNO_3$ (1.0 mmol) was added to a 3-ml DEAC (*N*,*N'*-Diethylacetamide) orange yellow solution of 0.5 mmol $(NH_4)_2WS_4$ and 0.5 mmol $Ca(NO_3)_2$, the dark precipitate was filtered off, and the red parallelepiped crystals were obtained after allowing the red filtrate to stand in air for one night: (anal.) $W_4Ag_6S_{16}CaO_6N_6C_{36}H_{78}$, (Calcd.) W, 28.00; H, 2.99; C, 16.46; N, 3.20, (found) W, 28.37; H, 3.05; C, 16.70; N, 3.60. IR (cm^{-1}): This polymeric complex displays DEAC vibration in the 4000–550 cm^{-1} range (19); W–(μ_n-S) ($n = 2, 3$): 505 w, 467 sh, 447 s, 436 s, 417 m; Raman (cm^{-1}): W–(μ_n-S) ($n = 2, 3$): 460 s, 449 m.

$\{[W_2Ag_2S_8]\cdot[Zn(4,4'\text{-bipy})_2(DMF)_2(DMSO)_2]\}_n$ **2**. Solution A: $AgNO_3$, (1 mmol) was added to a solution of 1 mmol $(NH_4)_2WS_4$ in 20 ml DMF and 4 ml DMSO, after all solids were dissolved, the dark precipitate was filtered off to give a red filtrate A.

Solution B: A 5-ml C_2H_5OH solution of 0.5 mmol 4,4′-bipy was added slowly to a stirring 8-ml C_2H_5OH and 2-ml acetone solvent mixture containing 0.5 mmol $Zn(ClO_4)_2$ for 15 min to afford a colorless solution B.

Solution A was put in a test tube then covered by solution B. 0.12 g red crystals were obtained after allowing the mixture to stand in air for four days: (anal.) $C_{10}H_{18}AgN_2O_2S_5WZn_{0.5}$, (Calcd.) C, 17.59; H, 2.66; N, 4.10; (found): C, 17.85; H, 2.80; N, 4.08. IR (cm^{-1}): ν_{CO}(DMF) 1641 (vs); ν_{SO}(DMSO): 957 m, 999 m; $\nu_{C-C, C-N}$: 1245–1066 m; ν_{C-H}: 2985–2921 w, δ_{C-H}: 1489–1378 m; W–S_t: 490 m; W–(μ_n-S) ($n = 2,3$): 442 s, 422 s. Raman (cm^{-1}): W–S_t: 489 m; W–(μ_n-S) ($n = 2, 3$): 464 s, 445 m; ν_s(Ag–S): 262 m, 242 m; δ(WS): 171 m.

TABLE 1
Crystal Data and Structure Refinement for Compounds 1, 2, 3

Complex	**1**	**2**	**3**
Empirical formula	$C_{36}H_{78}Ag_6CaN_6O_6S_{16}W_4$	$C_{10}H_{18}AgN_2O_2S_5WZn_{0.50}$	$C_{11}H_{23}NO_3WAgS_7Zn_{0.5}$
Formula weight	2626.70	682.97	766.13
Temperature	293(2)K	293(2)K	293(2)K
Wave length	0.71073 Å	0.71073 Å	0.71073 Å
Crystal system	Monoclinic	Monoclinic	Monoclinic
Space group	$P2_1/n$	$C2/c$	$C2/c$
Unit cell dimensions	$a = 13.769(3)$ Å	$a = 8.996(2)$ Å	$a = 28.8896(2)$ Å
	$b = 11.613(2)$ Å $\beta = 96.31(3)°$	$b = 21.728(4)$ Å $\beta = 94.00(3)°$	$b = 11.93950(10)$ Å
			$\beta = 122.9320(10)$
	$c = 24.153(5)$ Å	$c = 21.560(4)$ Å	$c = 16.2341(2)$ Å
Volume, Z	3838.7(13) Å^3, 2	4204(2) Å^3, 8	4699.82(8) Å^3, 8
Density (calculated)	2.273 Mg/m^3	2.158 Mg/m^3	2.166 Mg/m^3
Absorption coefficient	8.000 mm^{-1}	7.456 mm^{-1}	6.855 mm^{-1}
Diffractometer	Enraf–Nonius CAD4	Enraf–Nonius CAD4	Siemens Smart CCD
$F(000)$	2476	2592	2944
Crystal size	0.5 × 0.2 × 0.15 mm	0.70 × 0.25 × 0.20 mm	0.3 × 0.1 × 0.1 mm
Theta range for data collection	1.63 to 25.98°	1.87 to 26.00°	1.68 to 25.04°
Reflections collected	7700	4233	11447
Independent reflections	7517 [R(int) = 0.0273]	4121 [R(int) = 0.0385]	4119 [R(int) = 0.0254]
Refinement method	Full-matrix least-squares on F^2	Full-matrix least-squares on F^2	Full-matrix least-squares on F^2
Data/restraints/parameters	7501/0/340	4121/0/197	4119/0/206
Goodness-of-fit on F^2	1.009	1.066	1.027
Final R indices[$I > 2\sigma(I)$]	$R1 = 0.0607$, $wR2 = 0.1338^{a,b}$	$R1 = 0.0546$, $wR2 = 0.1556^{a,b}$	$R1 = 0.0438$, $wR2 = 0.1166^{a,b}$
R indices (all data)	$R1 = 0.1288$, $wR2 = 0.1763$	$R1 = 0.0722$, $wR2 = 0.1639$	$R1 = 0.0516$, $wR2 = 0.1218$
Largest diff. Peak and hole	0.769 and −1.684 eÅ^{-3}	2.123 and −1.686 eÅ^{-3}	3.801 and −2.024 eÅ^{-3}
Software	MolEN, SHELXTL-93	MolEN, SHELXTL-93	SHELXTL-93

[a] $R = \sum(\|F_o| - |F_c\|)/\sum|F_o|$.
[b] $wR2 = \{\sum w([(F_o^2 - F_c^2)^2/\sum w[(F_o^2)^2]\}^{1/2}$; for complex **1**: $w = [\sigma^2(F_o^2) + (0.0623P)^2]^{-1}$, where $P = (F_o^2 + 2F_c^2)/3$ for complex **2**: $w = [\sigma^2(F_o^2) + (0.0923P)^2 + 40.0859P]^{-1}$, where $P = (F_o^2 + 2F_c^2)/3$ for complex **3**: $w = [\sigma^2(F_o^2) + (0.0597P)^2 + 90.2574P]^{-1}$, where $P = (F_o^2 + 2F_c^2)/3$.

$\{[W_2Ag_2S_8]\cdot[Zn(4,4'\text{-}bipy)_2(DMSO)_4]\cdot(DMSO)\}_n$ **3**. $AgNO_3$ (1 mmol) was added to a solution of $(NH_4)_2WS_4$ (1 mmol) in 60 ml DMF and DMSO (v/v 5 : 1). After filtration, $Zn(ClO_4)_2$ (0.5 mmol) and 4,4′-bpy (0.5 mmol) was added into the filtrate, the resulting solution was allowed to stand in air for 2 h and then filtered again, 0.2 g orange crystals of **3** were obtained by allowing the solution to stand in air for one day: (anal.) $C_{11}H_{23}AgNO_3S_7WZn_{0.5}$; (calcd.) C, 17.25; H, 3.03; N, 1.83; (found) C, 17.31; H, 3.10; N, 1.91. IR (KBr pellet, cm^{-1}): ν_{SO}(DMSO): 1000.9 s; W–(μ_2-S): 447.4 s, 403.0 w.

X-Ray Structural Analysis

Crystal data collection and refinement parameters are given in Table 1. Selected atomic coordinates and equivalent isotropic displacement parameters are listed in Table 2. The intensity data of compounds **1** and **2** were collected at room temperature on an Enraf–Nonius CAD4 diffractometer using graphite monochromatized Mo$K\alpha$ radiation, and the diffraction data for compound **3** were collected on a Siemens Smart CCD area-detector diffractometer using graphite monochromatized Mo radiation. All calculations were performed by the MoLEN (20) and SHELXL 93 (21) program package. Both structures were solved by the heavy-atom method. Successive least-squares refinements and difference Fourier calculations revealed the positions of the remaining atoms. There was no attempt to add H atoms. The structures were refined by full-matrix least-squares on F^2.

TABLE 2
Selected Atomic Coordinates ($\times 10^4$) and Equivalent Isotropic Displacement Parameters ($A^2\times 10^3$) for 1, 2, 3

Atoms	X	Y	Z	U(eq)
		$\{[W_4Ag_6S_{16}]\cdot[Ca(DEAC)_6]\}_n$, **1**		
W(1)	864(1)	652(1)	1875(1)	58(1)
W(2)	4694(1)	638(1)	3286(1)	51(1)
Ag(1)	454(1)	−1832(1)	1885(1)	92(1)
Ag(2)	2749(1)	684(1)	2616(1)	90(1)
Ag(3)	4236(1)	−1835(1)	3294(1)	86(1)
S(11)	716(3)	1488(4)	1060(2)	77(1)
S(12)	−560(3)	−88(3)	1995(2)	78(1)
S(13)	1222(3)	1904(3)	2569(2)	70(1)
S(14)	2024(3)	−670(3)	1832(2)	92(2)
S(21)	5261(3)	1852(3)	3919(2)	76(1)
S(22)	3329(3)	−97(3)	3573(2)	68(1)
S(23)	4424(3)	1462(3)	2442(2)	64(1)
S(24)	5823(3)	−659(3)	3220(2)	73(1)
		$\{[W_2Ag_2S_8]\cdot[Zn(4,4'\text{-bipy})_2(DMF)_2(DMSO)_2]\}_n$, **2**		
W(1)	2321(1)	5108(1)	1600(1)	49(1)
Ag(1)	5000	5131(1)	2500	61(1)
Ag(2)	0	4998(1)	2500	86(1)
S(14)	4437(3)	4642(1)	1446(1)	54(1)
S(13)	2408(3)	5672(2)	2468(1)	55(1)
S(12)	1808(8)	5737(3)	843(2)	134(2)
S(11)	631(5)	4387(3)	1585(3)	130(2)
		$\{[W_2Ag_2S_8]\cdot[Zn(4,4'\text{-bipy})_2(DMSO)_4]\cdot(DMSO)\}_n$, **3**		
W	2612(1)	13290(1)	2618(1)	33(1)
Ag	2529(1)	15803(1)	2539(1)	54(1)
S(1)	3279(1)	12125(2)	2596(2)	53(1)
S(2)	1858(1)	12427(2)	1474(2)	51(1)
S(3)	2395(2)	14292(2)	3500(2)	62(1)
S(4)	2907(1)	14344(2)	1883(2)	46(1)

Note. U(eq) is defined as one third of the trace of the orthogonalized U_{ij} tensor.

DISCUSSION

Crystal Structure

$\{[W_4Ag_6S_{16}]\cdot[Ca(DEAC)_6]\}_n$ (DEAC = N,N′-diethylacetamide) 1, a novel hanging ladder-like polymeric chain. Compound **1** crystallizes in the monoclinic space group $P2_1/n$ (see Table 1). An ORTEP drawing of a segment of the anion in **1** is shown in Fig. 1. The polymeric anion can be viewed as a hanging ladder chain or a chain constructed of edge-sharing distorted square units extended along [0 1 0] direction. The mean W–Ag distance 2.960(10) Å in **1** is shorter than the corresponding values in discrete molecules, such as 2.971 Å in $[WS_4Ag_2(PPh_3)_3\cdot 0.8CH_2Cl_2]$ (22), 2.997 Å in $[W_2S_8Ag_4(PPh_3)_4]$ (23), 3.080 Å in $[WS_4Ag_3(PPh_3)_3(S_2P(OCH_2CH_3)_2]$ (24), which sugests that there is a continued slight W–Ag interaction in the chain. The average W–Ag distance of 2.960(10) Å in **1** is similar to those reported, such as 2.964 Å in $[W_4Ag_5S_{16}\cdot Nd(DMF)_8]_n$ (13) and 2.97(3) Å in $\{W_8Ag_{10}S_{32}\cdot[Nd(DMF)_8]_2\}$ (12). All metal atoms are coordinated by two μ_2-S and two μ_3-S with approximately tetrahedral geometry (with the angles S–W–S 105.1(2) ∼ 113.1(2)°, S–Ag–S 90.74(13) ∼ 126.3(12)°). The average lengths of W–μ_2-S, W–μ_3-S bonds are 2.18(1), 2.237(7) Å (see Table 3), which are comparable with those in other polymeric complexes, such as 2.190, 2.248 Å in $[W_4Ag_5S_{16}\cdot Nd(DMF)_8]_n$ (13), 2.189(9) and 2.23(1) Å in $\{W_8Ag_{10}S_{32}\cdot[Nd(DMF)_8]_2\}$ (12). The average W–Ag–W

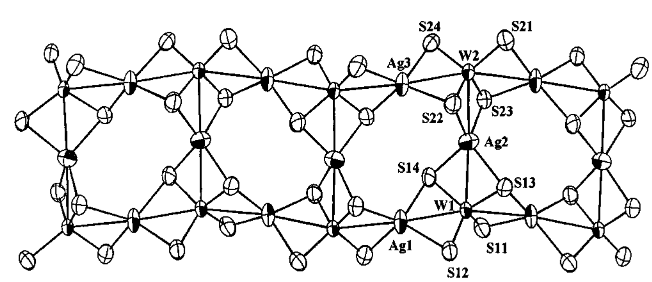

FIG. 1. ORTEP drawing of a portion of the polymeric anion of **1** $\{[W_4Ag_6S_{16}]\cdot[Ca(DEAc)_6]\}_n$ with atomic labeling (50% probability ellipsoids).

TABLE 3
Selected Bond Lengths (Å) and Bond Angles (deg) for Compounds 1, 2, 3

$\{[W_4Ag_6S_{16}]\cdot[Ca(DEAC)_6]\}_n$, **1**			
W(1)–S(11)	2.183(5)	W(2)–S(21)	2.163(4)
W(1)–S(12)	2.190(4)	W(2)–S(24)	2.183(4)
W(1)–S(14)	2.226(4)	W(2)–S(22)	2.243(4)
W(1)–S(13)	2.233(4)	W(2)–S(23)	2.244(4)
W(1)–Ag(1)	2.940(1)	W(2)–Ag(3)	2.941(1)
W(1)–Ag(2)	2.986(2)	W(2)–Ag(2)	2.974(2)
Ag(1)–S(12)	2.491(4)	Ag(2)–S(13)	2.527(4)
Ag(1)–S(23)#2	2.556(4)	Ag(2)–S(22)	2.531(5)
Ag(1)–S(14)	2.563(5)	Ag(2)–S(23)	2.555(4)
Ag(1)–S(21)#2	2.580(5)	Ag(2)–S(14)	2.576(5)
Ag(3)–S(11)#2	2.492(4)		
Ag(3)–S(22)	2.504(4)	Ca–O(1)	2.29(1)
Ag(3)–S(13)#2	2.569(4)	Ca–O(2)	2.25(1)
Ag(3)–S(24)	2.599(4)	Ca–O(3)	2.31(1)
Ag(1)–W(1)–Ag(3)#1	165.11(5)	Ag(3)–W(2)–Ag(2)	80.81(4)
Ag(3)–W(2)–Ag(1)#1	162.79(5)	Ag(1)#1–W(2)–Ag(2)	82.10(4)
W(1)–Ag(1)–W(2)#2	168.39(6)	Ag(1)–W(1)–Ag(2)	99.33(4)
W(2)–Ag(2)–W(1)	175.82(6)	Ag(3)#1–W(1)–Ag(2)	95.45(4)
W(2)–Ag(3)–W(1)#2	166.58(6)		
(Symmetry transformations used to generate equivalent atoms: #1, $-x+1/2$, $y+1/2$, $-z+1/2$; #2, $-x+1/2$, $y-1/2$, $-z+1/2$; #3 $-x-1$, $-y$, $-z$)			
$\{[W_2Ag_2S_8]\cdot[Zn(4,4'\text{-bipy})_2(DMF)_2(DMSO)_2]\}_n$, **2**			
W(1)–S(12)	2.154(5)	Ag(2)–S(11)	2.481(5)
W(1)–S(11)	2.180(4)	Ag(2)–S(11)#3	2.481(5)
W(1)–S(14)	2.203(3)	Ag(2)–S(13)	2.617(3)
W(1)–S(13)	2.235(3)	Ag(2)–S(13)#3	2.617(3)
W(1)–Ag(2)	2.9576(9)	Ag(2)–W(1)#3	2.9576(9)
W(1)–Ag(1)	2.987(1)	Zn(1)–O(2)#2	2.091(7)
Ag(1)–S(14)	2.528(3)	Zn(1)–O(2)	2.092(7)
Ag(1)–S(14)#1	2.528(3)	Zn(1)–O(1)	2.115(6)
Ag(1)–S(13)#1	2.609(3)	Zn(1)–O(1)#2	2.115(6)
Ag(1)–S(13)	2.609(3)	Zn(1)–N(1)#2	2.152(7)
Ag(1)–W(1)#1	2.987(1)	Zn(1)–N(1)	2.152(7)
O(1)–Zn(1)–O(1)#2	180.0	O(2)#2–Zn(1)–O(2)	180.0
O(2)–Zn(1)–N(1)	89.4(3)	O(2)#2–Zn(1)–O(1)	87.3(3)
O(1)–Zn(1)–N(1)	89.7(3)	O(2)–Zn(1)–O(1)	92.7(3)
N(1)#2–Zn(1)–N(1)	180.0		
(Symmetry transformations used to generate equivalent atoms: #1, $-x+1$, y, $-z+1/2$; #2, $-x+1/2$, $-y+1/2$, $-z$; #3, $-x$, y, $-z+1/2$)			
$\{[W_2Ag_2S_8]\cdot[Zn(4,4'\text{-bipy})_2(DMSO)_4]\cdot(DMSO)\}_n$, **3**			
W–S(4)	2.199(2)	W–S(1)	2.200(2)
W–S(3)	2.203(3)	W–S(2)	2.204(2)
W–Ag#1	2.9890(8)	W–Ag	3.0073(7)
Ag–S(2)#2	2.525(3)	Ag–S(3)	2.549(3)
Ag–S(4)	2.575(2)	Ag–S(1)#2	2.579(3)
Ag–W#2	2.9890(7)	Ag#1–S(1)	2.580(3)
Ag#1–S(2)	2.525(2)		
O(1)#3–Zn–O(1)	174.4(4)	O(1)#3–Zn–O(2)	93.4(3)
O(1)–Zn–O(2)	90.4(3)	O(1)#3–Zn–O(2)#3	90.4(3)
O(1)–Zn–O(2)#3	93.4(3)	O(2)–Zn–O(2)#3	95.5(5)
O(1)#3–Zn–N#3	90.4(3)	O(1)–Zn–N#3	85.7(3)
O(2)–Zn–N#3	86.5(3)	O(2)#3–Zn–N#3	177.8(3)
O(1)#3–Zn–N	85.7(3)	O(1)–Zn–N	90.4(3)
O(2)–Zn–N	177.8(3)	O(2)#3–Zn–N	86.5(3)
N#3–Zn–N	91.5(4)		
(Symmetry transformations used to generate equivalent atoms: #1, $-x+1/2$, $y-1/2$, $-z+1/2$; #2, $-x+1/2$, $y+1/2$, $-z+1/2$; #3, $-x+1$, y, $-z+3/2$)			

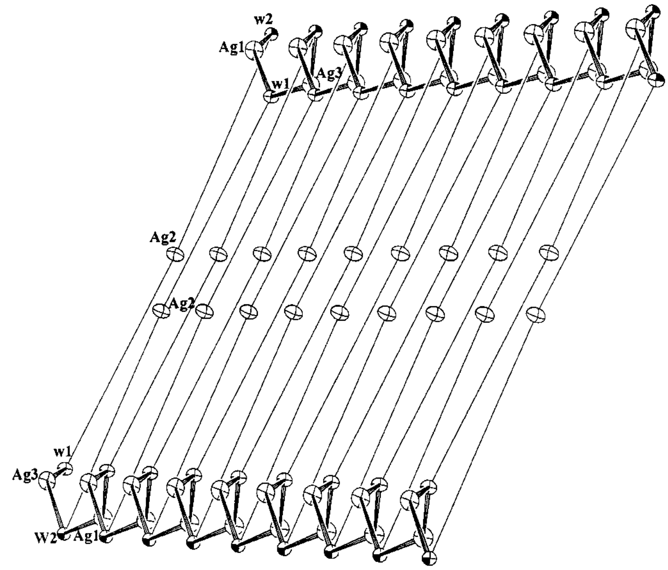

FIG. 2. Simplified diagram of the double-stranded helical chain of **1**. For clarity, the sulfur atoms are omitted.

angle for complex **1** is 170.3(2)°, Ag–W–Ag in a square unit is 89.4(2)°, and Ag–W–Ag between two square units is 163.95(10)°, which are similar to those reported, such as 173(2), 87(1), 174(3) in $\{[W_4Ag_5S_{16}]_2\cdot La(DEF)_2(DMF)_6 La(DEF)_4(DMF)_4]_n$ (14).

The anion chain of complex **1** is also characterized as a double-stranded chain (Fig. 2), which is propagated along the crystallographic *b* axis. It can be seen that two helixes are bridged together by Ag2 atoms. The distance between the two helixes is 5.96 Å. Each helix has a repeat unit $(W_2Ag_2S_8)^{2-}$, and is defined by a pitch (length per turn) of 11.61 Å and a radius of 5.86 Å (Ag1–Ag3: 5.84 Å, W2–W1: 5.88 Å).

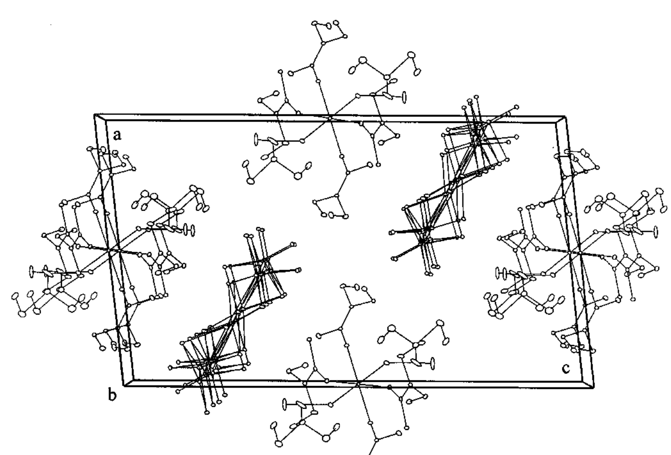

FIG. 3. Packing diagram of **1** down *b* axis.

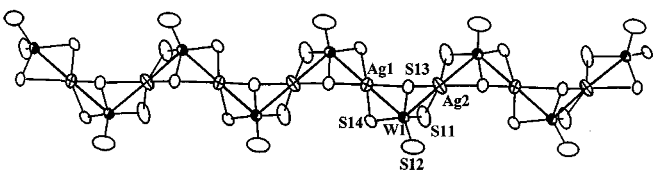

FIG. 4. ORTEP diagram of the zigzag anionic chain of **2** (thermal ellipsoids at the 50% probability level).

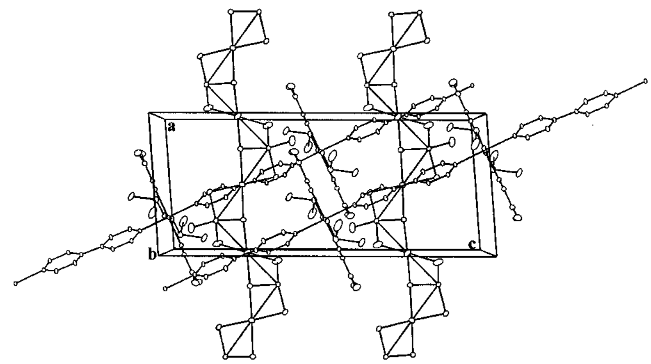

FIG. 6. Packing diagram of **2** down the *b* axis.

Each Ca^{II} is coordinated by six DEAC molecules. The $Ca–O_{(av)}$ bond length in **1** is 2.288(38) Å. Figure 3 shows the packing diagram of compound **1** down the *b* axis.

$\{[W_2Ag_2S_8]\cdot[Zn(4,4'\text{-}bipy)_2(DMF)_2(DMSO)_2]\}_n$ **2**, *a novel composite polymer containing a zigzag anionic chain and a linear cationic chain.* The zigzag anionic chain in compound **2** is extended along the [1 0 0] direction while the linear cationic chain is extended along [1 0 1] direction (see Figs. 4 and 5).

W1 is coordinated by one μ_t-S, two μ_2-S and one μ_3-S. The S–W–S angle ranges from 106.0(2) to 109.5(3)°. The mean bond lengths of W–μ_t-S, W–μ_2-S, and W–μ_3-S are 2.154(5), 2.19(1), and 2.235(3) Å, respectively. In comparison, the bond lengths are 2.146, 2.199 and 2.250 Å in a zigzag chain complex $[W_4S_{16}Ag_4\cdot 2Ca(DMSO)_6]_n$ (10). The $[AgS_4]$ tetrahedron is distorted with an S–Ag–S angle range of 92.42(12) ~ 130.3(2)°, and the Ag–S mean distance is 2.56(5) Å, which are simlar to those value in $[W_4S_{16}Ag_4\cdot 2Ca(DMSO)_6]_n$ (10), 91.3 ~ 123.5°, 2.56 Å. The $[WS_4]$ tetrahedron shares an edge with the $[AgS_4]$ tetrahedron.

As shown in Fig. 4, the angles of Ag1–W1–Ag2, W–Ag1–W, and W–Ag2–W are 98.61(2), 178.11(6), and 170.80(8)°, respectively. The W–Ag mean distance is 2.97(1) Å. For comparison, the average angle of Ag–W–Ag at coners is 93.7° and the average angle of W–Ag–W is 173.6°, the mean W–Ag distance is 2.969 Å in $[W_4S_{16}Ag_4\cdot 2Ca(DMSO)_6]_n$ (10).

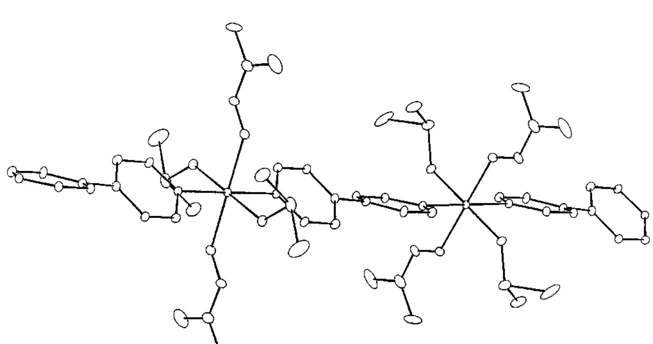

FIG. 5. ORTEP diagram of the linear cationic chain in **2** (thermal ellipsoids at the 10% probability level).

The 1-D linear cationic chain in **2** is extended along [1 0 1] direction. The Zn atom is octahedrally coordinated by two DMSO molecules, two DMF molecules, and two N atoms from two 4,4′-bipy molecules with the angles between 87.3(3)° and 180.0°. The Zn–O distance is 2.10(1) Å, and the Zn–N distance is 2.152(7) Å.

Figures 6 and 7 show the packing diagram of **2** down *b* and *a* axes. Selected bond lengths and angles are listed in Table 3.

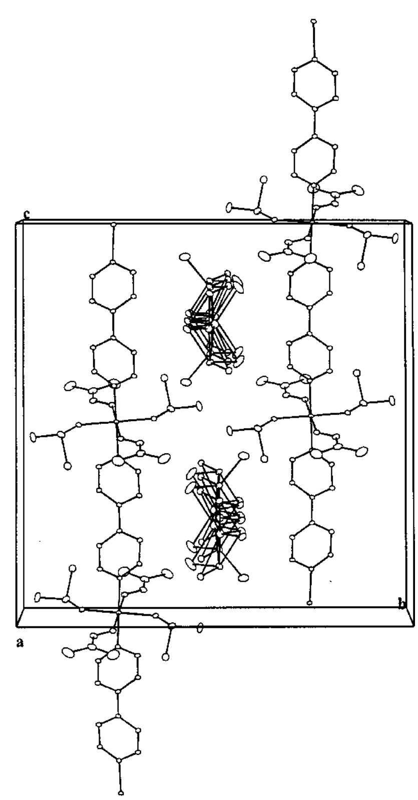

FIG. 7. Packing diagram of **2** down the *a* axis.

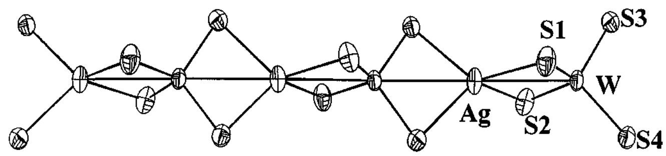

FIG. 8. ORTEP drawing of a portion of the anion of **3** (thermal ellipsoids at the 50% probability level).

$\{[W_2Ag_2S_8]\cdot[Zn(4,4'\text{-}bipy)_2(DMSO)_4]\cdot(DMSO)\}_n$ **3**, *a novel composite polymer contains a linear anionic chain and a zigzag cationic chain.* The linear anionic chain in compound **3** is extended along [0 1 0] direction while the zigzag cationic chain is extended along [0 0 1] direction. The linear anionic and zigzag cationic chains of this complex are shown in Figs. 8 and 9 together with the packing diagram of the unit cell shown in Fig. 10. The selected geometric parameters are listed in Table 3.

This complex consists of both polymeric anions and polymeric cations. The polymeric anionic chain has distorted and tetrahedrally coordinated Ag and W atoms with the angles ranging from 90.80(8) to 126.67(6)°, and the chain is deviated from linear configuration with the W–Ag–W angle 177.18(3)° and the Ag–W–Ag angle 169.57(1)°, respectively. For comparsion, the angles are 177.1, 177.1° in $[WS_4Ag\cdot HNEt_3DMF]_n$ (8), and 180.0, 180.0° in $[WS_4Ag\cdot NH_4]_n$ (13). The average W–μ_2-S, Ag–μ_2-S bonds, and W–Ag distances are 2.201(2), 2.56(2), and 2.995(8) Å, respectively, which are simlar to those data in other liner polymeric complexes, e.g., 2.202, 2.546, 2.983 Å in $[WS_4Ag\cdot HNEt_3DMF]_n$ (8), 2.212, 2.533, 2.928 Å in $[WS_4Ag\cdot NH_4]_n$ (13).

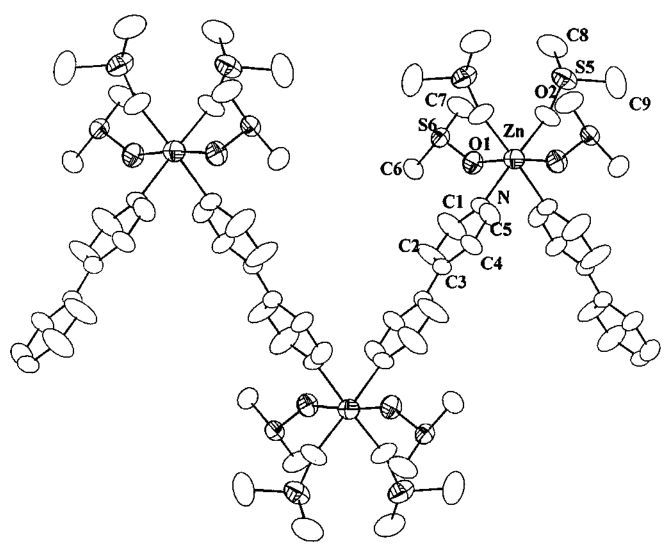

FIG. 9. ORTEP drawing of a portion of the cation of **3** (thermal ellipsoids at the 50% probability level).

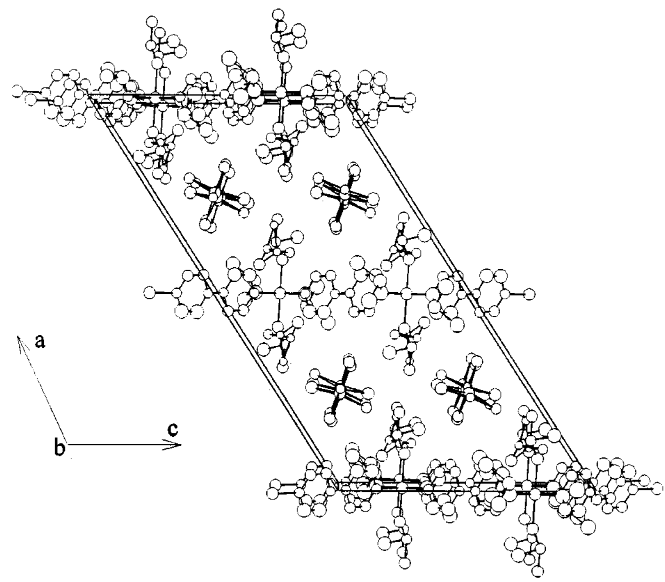

FIG. 10. Packing drawing of the unit cell of **3** down the *b* axis.

The polymeric cation has a zigzag configuration with the N–Zn–N angle of 91.5(4)° which is close to 90° (see Fig. 9). The Zn atom is octahedrally coordinated by four DMSO molecules and two N atoms from two 4,4′-bipy molecules with the angles between 85.7(3) and 95.5(5)°. The Zn–O, Zn–N bonds are 2.16(2) and 2.297(7) Å, respectively, which are substantially longer than those of 2.10(1) and 2.152(7) in **2** due to the four large coordinate DMSO molecules.

Electrical Properties

(1) *Electrical conductivity.* The electrical conductivities of complexes **1**–**3** were measured with pressed pellets (two probes). The conductivity is a function of temperature (Schemes 1 and 2). The conductivity of compound **3** is less

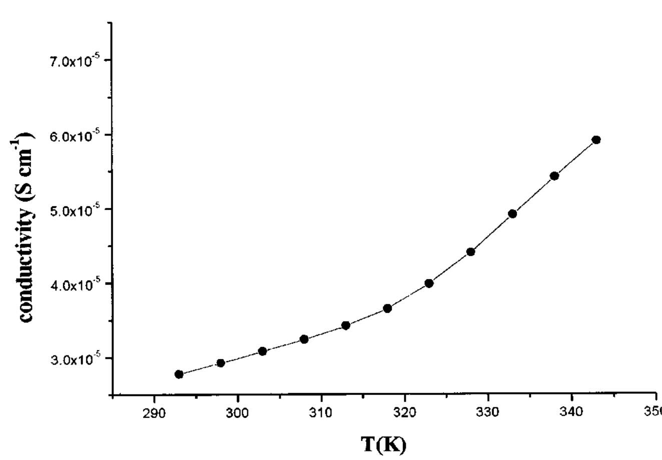

SCHEME 1. The conductivity of **1** is a function of temperature.

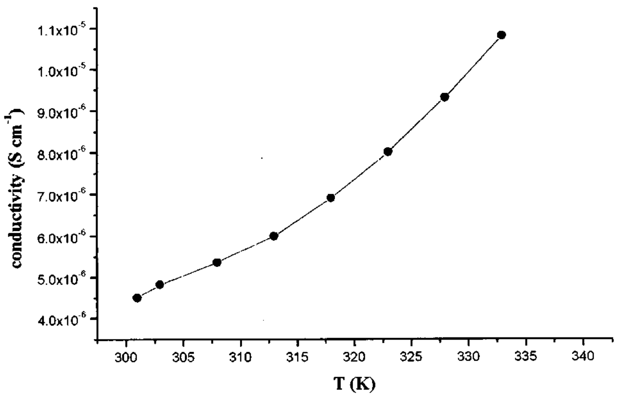

SCHEME 2. The conductivity of **2** is a function of temperature.

TABLE 4
Atom Parameters in EHT Calculation

Atom	Obital	H_{ii}(eV)	$\zeta_{11}(c_1)$	$\zeta_{12}(c_1)$
W	6*s*	− 8.260	2.341	
	6*p*	−5.170	2.309	
	5*d*	−10.370	4.982(0.6940)	2.068(0.5631)
Ag	5*s*	−11.100	2.244	
	5*p*	−5.800	2.202	
	4*d*	−14.500	6.070(0.5591)	2.663(0.6047)
S	3*s*	−22.00	2.122	
	3*p*	−13.3	1.827	

than 10^{-8} S cm^{-1}, which is out of the test range of the conductometer. According to the definition of Kittel (25), the conductivity of semiconductors is 10^{-9} to 10^{2} S cm^{-1}, complexes **1** and **2** belong to semiconductors.

The increase of these three compounds in conductivity is according to the order **1** > **2** > **3**. From the experiments, it can be concluded that the conductivities of these compounds are related to the charge density of the anionic repeat unit. The conductivities of **3**, **2**, **1** are increased, which is in good agreement with their structural characteristics.

(2) *Electronic band structure.* The band of these polymers have been calculated by the EHT crystal orbital method (26–28). Their energy gaps (Eg) of **1**, **2**, **3** are 3.70, 3.87, and 3.93 (eV), respectivly, which are in the range of semiconductors (Table 4, Fig. 11). It is shown that the characters of the top of valence-band are bond orbital between the Ag atoms and S atoms, and the bottom of conductor-band consists of the antibonds between the W atoms and the S atoms. Therefore, under the electric field or optical excitation, electrons can transfer from the Ag atom to the W atom and then to the Ag atom; and μ_2-S, μ_3-S have influence on the conductibility of these complexes, while the influence of μ_t-S is not so obvious. The energy gaps (Eg) of **3**, **2**, **1** are decreased, which is in good agreement with their conductivities and structural characteristics.

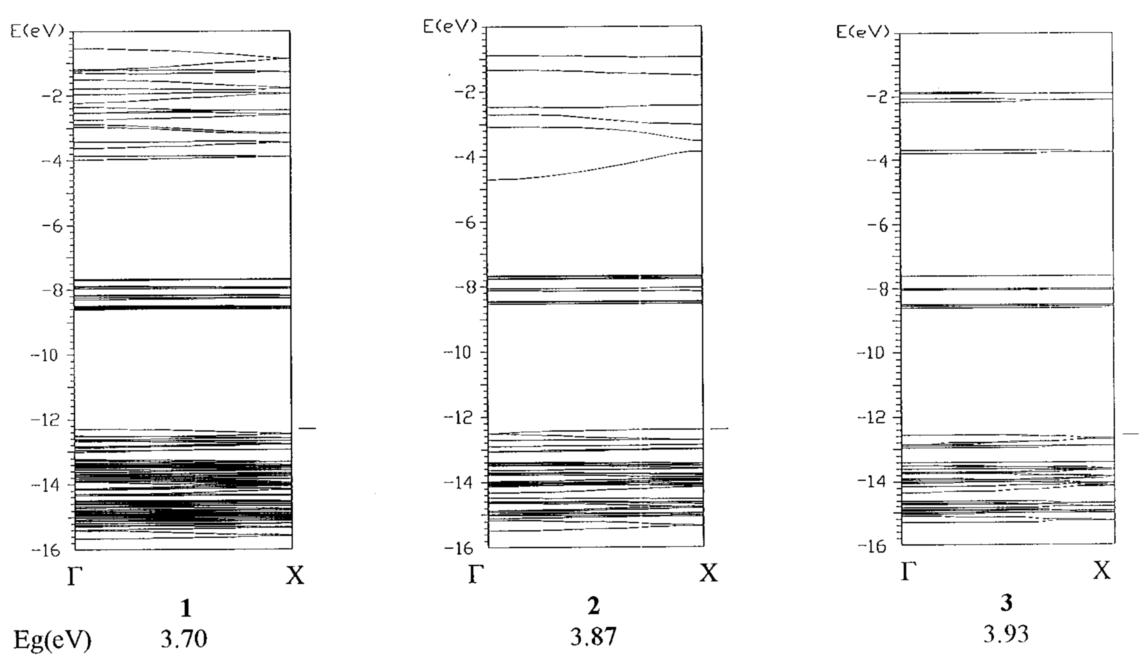

FIG. 11. Electronic band structure of **1**, **2**.

ACKNOWLEDGMENTS

This research was supported by grants from the State Key Laboratory of Structural Chemistry, Fujian Institute of Research on the Structure of Matter, the Chinese Academy of Sciences, the National Science Foundation of China, and the Science Foundation of CAS and Fujian Province.

REFERENCES

1. M. Fujita, Y. J. Kwon, S. Washizu, and K. Ogura, *J. Am. Chem. Soc.* **116,** 1151 (1994).
2. A. Aumuller, P. Erk, G. Klebe, S. Hünig, J. U. von Schütz, and H.-P. Werner, *Angew. Chem. Int. Ed. Engl.* **25,** 740 (1986).
3. (a) A. Müller, F. Peters, M. I. Pope, and D. Gatteschi, *Chem. Rev.* **98**(1), 239 (1998). (b) A. Müller, Jochen Meyer, Erich Krickemeyer, Christian Beugholt, *et al.*, *Chem. Eur. J.* **4**(6), 1000 (1998).
4. E. Coronado and C. J. Gomes-Carcia, *Chem. Rev.* **98**(1), 273 (1998).
5. D. E. Katsoulis, *Chem. Rev.* **98**(1), 359 (1998).
6. E. I. Stiefel and K. Matsumoto, *in* "Transition Metal Sulfur Chemistry: Biological and Industrial Significance." Chap. 1, pp. 2–39; Chap. 17, pp. 282–296; Chap. 20, pp. 324–335. American Chemical Society, Washington, DC, 1996.
7. (a) A. Müller, W. Jaegermann, and W. Hellmann, *J. Mol. Struct.* **100,** 559 (1983); (b) A. Müller and W. Hellmann, *Spectrochim. Acta A* **41,** 359 (1985); (c) J. P. Lang, J. G. Li, S. A. Bao, and X. Q. Xin, *Polyhedron* **12**(7), 801 (1993).
8. (a) Q. Huang, X. T. Wu, T. L. Sheng, and Q. M. Wang, *Acta Crystallogr. Sect. C* **52,** 29 (1996); (b) Q. Huang, X. T. Wu, T. L. Sheng and Q. M. Wang, *Acta Crystallogr. Sect. C* **52,** 795 (1996).
9. Q. Huang, X. T. Wu, T. L. Sheng, and Q. M. Wang, *Inorg. Chem.* **34,** 4931 (1995).
10. Q. Huang, X. T. Wu, and J. X. Lu, *Inorg. Chem.* **35,** 7445 (1996).
11. Q. Huang, X. T. Wu, and J. X. Lu, *Chem. Commun.* 703 (1997).
12. L. Chen, X. T. Wu, X. C. Gao, W. J. Zhang, and P. Lin, *J. Chem. Soc. Dalton Trans.* 4303 (1999).
13. Q. Huang, X. T. Wu, Q. M. Wang, T. L. Sheng, and J. X. Lu, *Angew. Chem. Int. Ed. Engl.* **35**(8), 868 (1996).
14. L. Chen, X. T. Wu, and P. Lin, *J. Chem. Crystallogr.* **29**(5), 629 (1999).
15. G. C. Papavassiliou, *Prog. Solid Sate Chem.* **25,** 125 (1997).
16. *Chem. Abstracts* **90**.
17. R. Flükiger, R. Baillif, and E. Walker, *Mats. Res. Bull.* **13,** 743 (1978).
18. J. W. McDonald, G. D. Friesen, L. D. RosenHein, and W. E. Mewton, *Inorg. Chim. Acta* **72,** 205 (1983).
19. (a) R. A. Nyquist and R. O. Kagel, Infrared spectra of inorganic compounds, (b) Inorganics IR grating spectra, SADTLER Research Laboratories, DEAC 333489K
20. (a) "MoLEN/PC Structure Determination Package." Enraf–Nonius, Delft, Holland, 1990; (b) J. D. Dunitz and P. Seiler, *Acta Crystallogr. Sect. B* **29,** 589 (1973).
21. Siemens, "SHELXTL Version 5 Reference Manual." Siemens Energy and Automation Inc., Madison, WI, 1994.
22. A. Müller, H. Bogge, and U. Shimanski, *Inorg. Chim. Acta* **69,** 5 (1983).
23. A. Müller, H. Bogge, and E. Koniger-Ahlborn, *J. Chem. Soc. Chem. Commun.* 739 (1978).
24. S. W. Du, N. Y. Zhu, P. C. Chen, and X. T. Wu, *J. Mol. Struc.* **291,** 167 (1993).
25. C. Kittel, "Solid State Physics," fifth ed., Wiley, New York, 1976.
26. R. Hoffmann, *J. Chem. Phys.* **39,** 1397 (1963).
27. J. K. Burdett and S. Lee, *J. Am. Chem. Soc.* **105,** 1079 (1983).
28. J. K. Burdett and T. J. Mclarnan, *Inorg. Chem.* **21,** 1119 (1982).